JOURNAL OF MORPHOLOGY 275:961–979 (2014)

Density and Distribution of Cutaneous Sensilla on Tails of Leopard Geckos (*Eublepharis macularius*) in Relation to Caudal Autotomy

Anthony P. Russell,[1]* Erica K. Lai,[1] G. Lawrence Powell,[1] and Timothy E. Higham[2]

[1]*Department of Biological Sciences, University of Calgary, 2500 University Drive NW, Calgary, Alberta, Canada T2N 1N4*
[2]*Department of Biology, University of California, 900 University Avenue, Riverside, California 92521*

ABSTRACT The lizard tail is well known for its ability to autotomize and regenerate. Physical contact of the tail by a predator may induce autotomy at the location at which the tail is grasped, and upon detachment the tail may undergo violent, rapid, and unpredictable movements that appear to be, to some degree, regulated by contact with the physical environment. Neither the mechanism by which tail breakage at a particular location is determined, nor that by which environmental feedback to the tail is received, are known. It has been suggested that mechanoreceptors (sensilla) are the means of mediation of such activities, and reports indicate that the density of sensilla on the tail is high. To determine the feasibility that mechanoreceptors are involved in such phenomena, we mapped scale form and the size, density, distribution, and spacing of sensilla on the head, body, limbs, and tail of the leopard gecko. This species has a full complement of autotomy planes along the length of the tail, and the postautotomic behavior of its tail has been documented. We found that the density of sensilla is highest on the tail relative to all other body regions examined; a dorsoventral gradient of caudal sensilla density is evident on the tail; sensilla are more closely spaced on the dorsal and lateral regions of the tail than elsewhere and are carried on relatively small scales; and that the whorls of scales on the tail bear a one to one relationship with the autotomy planes. Our results are consistent with the hypotheses of sensilla being involved in determining the site at which autotomy will occur, and with them being involved in the mediation of tail behavior following autotomy. These findings open the way for experimental neurological investigations of how autotomy is induced and how the detached tail responds to external environmental input. J. Morphol. 275:961–979, 2014.

KEY WORDS: epidermis; mechanoreception; tail loss; sensoty input; lizard; regeneration; movement; SEM

INTRODUCTION

Response to contact, and the modulation of movement, are often associated with complex feedback systems between an animal and its internal and external environments. Detection of external physical signals is often mediated through an array of receptors on the body, such as the lateral line system of fishes, whereby clusters of mechanosensory hair cells (neuromasts) permit detection of disturbances in the water. Such monitoring is important in ecologically relevant situations, such as predator avoidance (Stewart et al., 2013). Stimuli are filtered through the sensory apparatus, and the architecture of the receptor organ is important in determining how this filtering occurs (Sane and McHenry, 2009). Sensory receptors are also found on the bodies (and tails) of terrestrial vertebrates, such as lizards. Compared to aquatic organisms, much less is known about the role of these receptors in the modulation of movement and responses to contact via the abiotic environment or a potential aggressor.

Caudal autotomy is widespread among lizards and has been associated with defense against predation (e.g., Clark, 1971). The tail can either be released when grasped by the jaws of a predator, or it can be jettisoned without physical contact, in response to a visual stimulus (Werner, 2008). In both cases, if free of any encumbrance, the cast-off tail may undergo spontaneous movements that ostensibly attract the attention of the predator, thus allowing the lizard more time for escape (Arnold, 1984). Recent investigations of the movement of the detached tail have revealed that

Additional Supporting Information may be found in the online version of this article.

Contract grant sponsor: The Natural Sciences and Engineering Research Council of Canada (Discovery Grant funding; A.P.R.).

*Correspondence to: Anthony P. Russell, Department of Biological Sciences, University of Calgary, 2500 University Drive NW, Calgary, Alberta, Canada T2N 1N4. E-mail: arussell@ucalgary.ca

Received 19 December 2013; Revised 6 February 2014; Accepted 21 February 2014.

Published online 19 March 2014 in Wiley Online Library (wileyonlinelibrary.com).
DOI 10.1002/jmor.20269

simple cyclical, or more complex and randomized patterns of activity may be exhibited. In its simplest form the tail may exhibit only rhythmic swings, for which electromyographic (EMG) records reveal alternating, cyclic patterns of left-right muscle contraction that bend the tail from side to side (Rumping and Jayne, 1996), as for the detached tail of the Tokay gecko (*Gekko gecko*). Contrastingly, the autotomized tail of the leopard gecko (*Eublepharis macularius*) exhibits a combination of rhythmic swings (equivalent to the movements of the Tokay tail) and more vigorous and unpredictably timed jumps, flips, and lunges (Higham and Russell, 2010, 2012). This mixed pattern is now confirmed for the detached tails of other geckos (Higham et al., 2013a). Differential patterns of muscle activation bring about these two behaviors. The combination of stereotyped and nonstereotyped activities result in unpredictable patterns of motion (Higham et al., 2013a), enhancing the distraction of the predator.

The concept of economy of autotomy (Werner, 1964, 1968; Bustard, 1968; Daniels, 1985; Medel, 1992; Cooper and Smith, 2009) suggests that only the "necessary" amount of tail will be shed to enable escape from an aggressor. In many lizards capable of caudal autotomy, fracture planes are present within all postpygal vertebrae (Werner, 2008). How fracture is localized to a particular fracture plane is not known (Higham et al., 2013b), but sensory input at the site of contact with the tail (if such contact occurs), and local reflex circuitry, likely play predominant roles. The anchor point of contact (such as a predator's jaws) is often the trigger for release of the tail (Bellairs and Bryant, 1985), and breakage immediately anterior to the point of contact was demonstrated by Woodland (1920). Such observations are suggestive that economy of autotomy is mediated through sensory feedback. Fox et al. (1998) determined the pinching force necessary to induce autotomy in *Uta stansburiana*, which also implies mediation through sensory feedback.

Recognition of the existence of variable patterns of muscle contraction in the detached tail has raised the question of what neural networks are involved in their control (Higham and Russell, 2012). The rhythmic patterns have been shown to be consistent with the output of a central pattern generator (CPG) (Brown, 1911; Harris-Warrick and Johnson, 1989; Harris-Warrick and Marder, 1991; Yakovenko et al., 2005; Chevalier et al., 2008; Whelan, 2010). CPG-generated actions can be modulated via proprioceptive or exteroreceptive sensory feedback (Gottschall and Nicholls, 2007), although such feedback is not necessary to initiate or perpetuate them. Although the mechanisms underlying the more complex ballistic tail movements are yet to be determined (Higham and Russell, 2012), it is possible that they are controlled by independent neural pathways, such as multiple CPGs or possibly a non-CPG pathway. Whatever these mechanisms are, they appear to be differentially sensitive to feedback from the external environment (Higham and Russell, 2010, 2012). The additional neural output required for this could result from random patterns of firing until the muscles that the nerves control are fatigued (Higham et al., 2013a), because the ballistic actions are only produced for the first 90 s or so after autotomy (Higham and Russell, 2012). Available evidence, however, suggests that modulation is governed, at least in part, by interactions of the tail with the external environment.

During ballistic movements of the detached tail there are significant periods of coactivation between muscles of the left and right sides within the same segment, with only a very short delay in EMG activity between them. This contrasts with the alternating patterns that drive the rhythmic swings (Higham and Russell, 2010, 2012). When observed in a test arena, flips, and jumps of the detached leopard gecko tail occurred in the absence of contact with the arena walls, but lateral lunges resulted from such contact. Although the flips and jumps seemingly occurred without any obvious cue from the environment, it is evident that the detached tail remains dorsal side up most of the time, and is able to right itself if it inverts.

The role of sensory input in the modulation of the movement patterns of the detached tail (Higham et al., 2013a) remains unknown, although Mahendra (1936) noted that once the activity of the detached tail of *Hemidactylus flaviviridis* had subsided, tactile stimulus was able to rekindle its movements. Such observations indicate that sensory feedback is important for at least some of the movement of detached tails (Higham et al., 2013a). It has been proposed that epidermal sense organs on the surface of the tail are involved in its movement following autotomy (Higham et al., 2013b), and that deformation of the integumentary surface initiates firing of the associated nerves (Maclean, 1980). Matveyeva and Ananjeva (1995) noted that the integument of lizard tails is well endowed with mechanoreceptive sensilla, but proffered no explanation of why this might be so.

Sensilla are integumentary modifications of the heavily keratinized epidermis of squamates (Maderson, 1965), that manifest as circular depressions on the surface of scales, within which lies a raised central "button" (Hiller, 1978). They are found in many reptiles, and have been shown to have variable distribution patterns across the body (Bauer and Russell, 1988). Abundant aggregations of them are typically associated with labial scales, scales bordering the digits (Schmidt, 1913; Audy, 1953; Hiller, 1968; Schleich and Kästle, 1986), subdigital adhesive scansors (Audy, 1953; Lauff et al., 1993), and scales on the tail (Hiller, 1971; Bauer and Russell, 1988; Matveyeva and

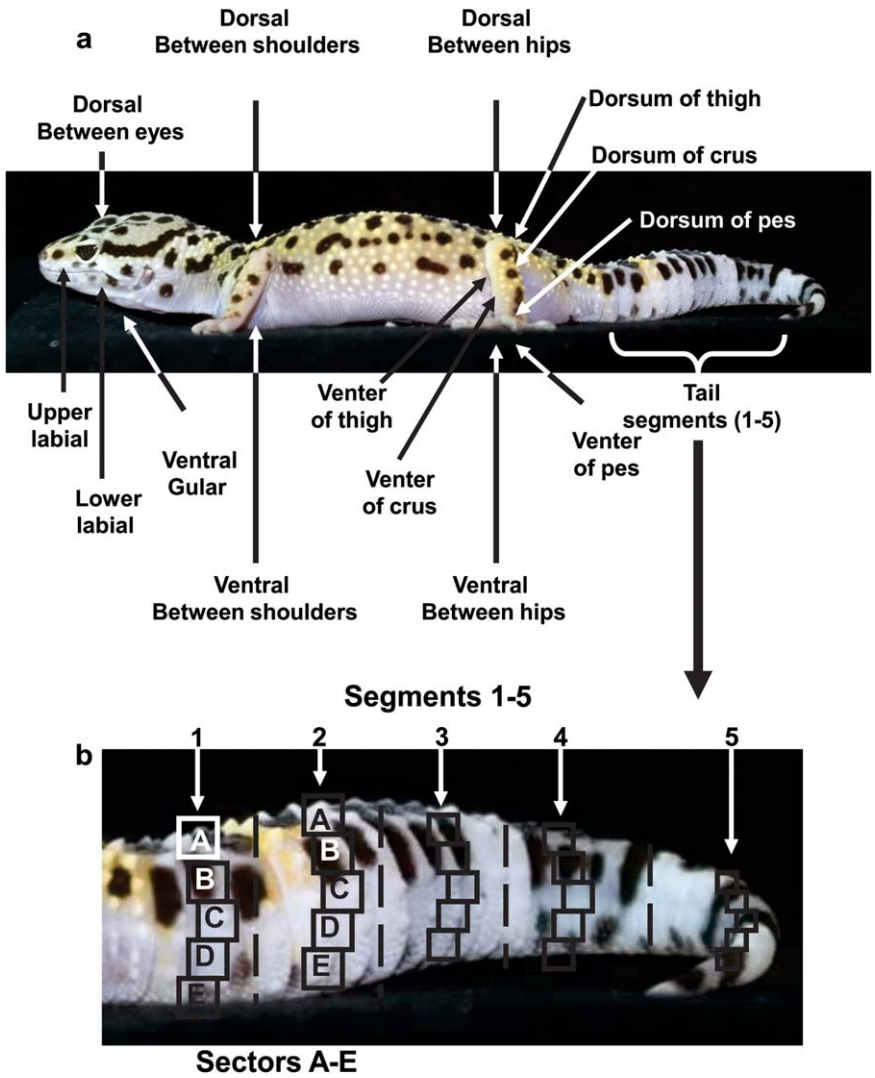

Fig. 1. Locations from which skin samples of *E. macularius* were taken. (**a**) Location of sampling areas for the body. (**b**) Location of sampling areas for the tail (original and regenerated). The tail was cut into five segments longitudinally (1–5), as indicated by the vertical, dashed lines, and from within each segment a strip of skin was removed and divided, from dorsal to ventral, into five sectors of equal area (A–E), as denoted by the boxes. The absolute area of the sectors diminished from anterior to posterior, in accordance with the tapering of the tail.

Ananjeva, 1995). Some sensilla bear bristles or hair-like projections, whereas others are glabrous and lens-shaped (Hiller, 1971; Stewart and Daniel, 1975; Ananjeva et al., 1991; Nikitina and Ananjeva, 2005). When the projections are moved or pressure is placed on the button of the sensillum, the intraepidermal sensory receptors (Miller and Kasahara, 1967) are deformed, and associated expanded tip-nerve terminals convert the mechanical stimulus into neural signals that are transmitted to the spinal cord (Iggo, 1982; Zimmermann, 1986; Eckert et al., 1988; Eisthen and Braun, 2001).

Cutaneous sense organs exhibit a wide range of form and complexity (Landmann, 1975). Their inferred mechanoreceptive role (Leydig, 1868; Cartier, 1872; Todaro, 1878; Schmidt, 1912, 1913; Bailey, 1969) was physiologically demonstrated by Hiller (1978). Analogous bristled receptors of insects (Zacharuk and Shields, 1991; Walters et al., 1998) and mites (Haupt and Coineau, 1978) have also been shown to be mechanoreceptive. The possibility of additional sensory capabilities of squamate integumentary receptors, such as thermoreception (Bailey, 1969; Ananjeva et al., 1991) or hydroreception (Matveyeva and Ananjeva, 1995), has not yet been demonstrated. The functionality of mechanoreceptive sensilla throughout ecdysis of both arthropods (Haupt and Coineau, 1978) and geckos (Hiller, 1976) indicates that proprioceptive sensitivity remains available at all times.

The cell bodies of the afferent nerves running from the cutaneous receptors of squamates reside in the dorsal root ganglia of the spinal cord (Whimster, 1980). This is of significance for caudal

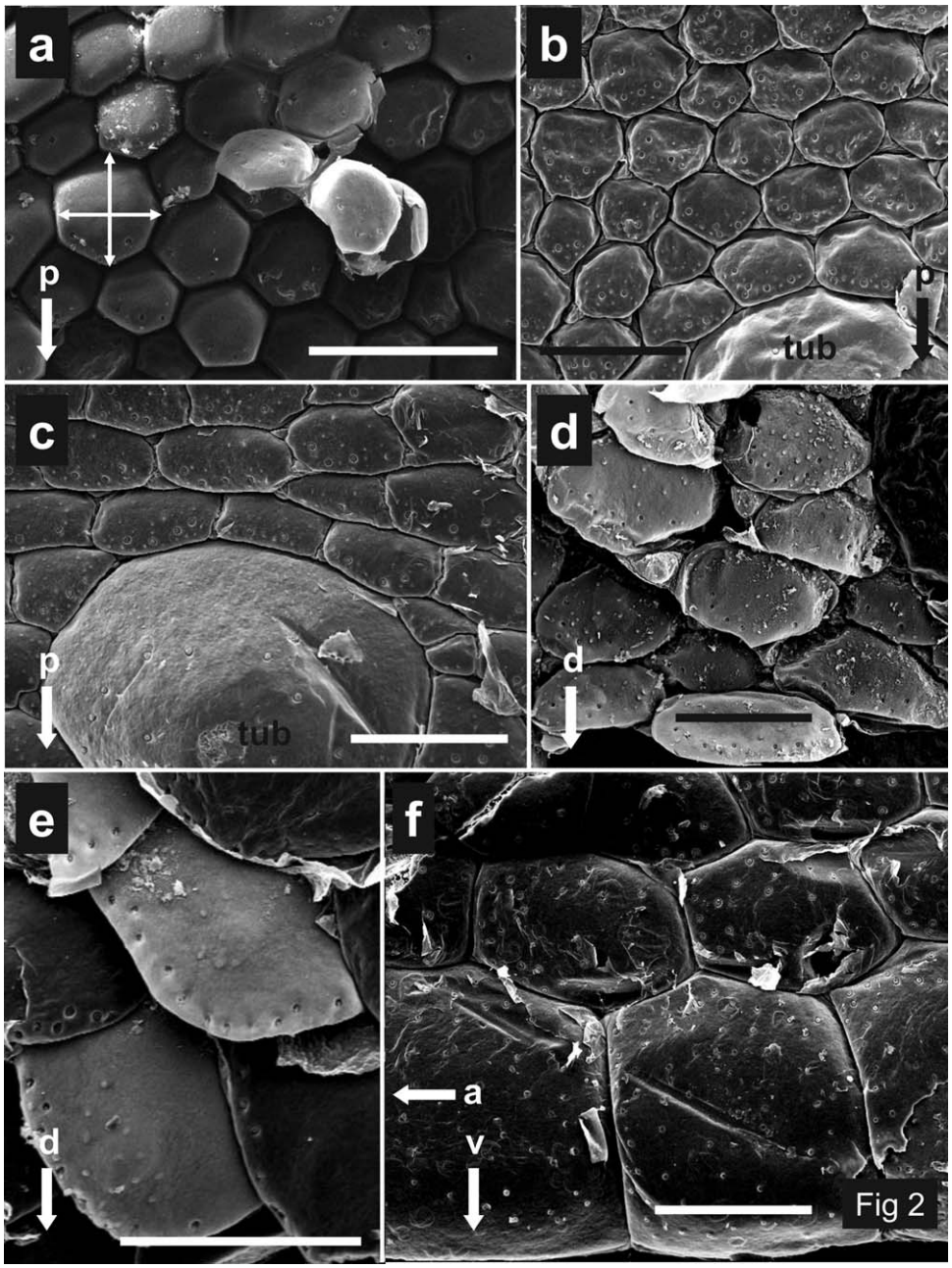

Fig. 2. Scales and their associated sensilla from the dorsal regions of the body (see Fig. 1a). (**a**) Head between the eyes. The white, double-headed arrows depict how the sizes of scales were recorded, by measuring the longest and shortest dimension of the scales in each area sampled. Note the lighter-colored scales in the center of the image—these still retain the outer epidermal generation that was stripped away from most of the scales during the cleaning process. Sensilla are evident as pits surrounding button-like mounds on the scales. (**b**) Between the shoulders. Part of a tubercle (tub) is evident at the bottom of this panel. (**c**) Between hips. A tubercle (tub) is prominently displayed at the bottom of this panel. (**d**) Thigh. (**e**) Pes. (**f**) Upper labial and, to the top of the panel, adjoining rostral scales. Sensilla are distributed across the surface of the labial scales. Directions are indicated by arrows—a, anterior; d, distal; p, posterior; v, ventral. The scale bar for all panels = 500 μm.

autotomy, because when the nerve cord is severed during the casting off of the tail, local reflex pathways remain intact, creating a naturally occurring spinal preparation (Rumping and Jayne, 1996; Higham and Russell, 2010), and providing the possibility for feedback from the environment within the isolated tail. Furthermore, when the tail regenerates, new sensory circuits must be established from the stump of the tail, recruiting dorsal root ganglia that lie proximal to the plane of autotomy. Because the regenerated tail has a different anatomy from the original (Gilbert et al., 2013), the pattern of distribution of the sensilla in the regenerated structure may be expected to differ from that of the original.

Given the evidence suggesting that external input is involved in the modulation of postautotomic tail movements of the leopard gecko, and may also be involved in determining where along the tail autotomy takes place, we predict that 1) the original tail will exhibit densities and distribution patterns of cutaneous sensilla that are consistent with the behavior patterns of the detached tail, and that are different from the patterns expressed on the body; 2) such sensilla of the original tail will exhibit differential patterns of distribution dorsoventrally, and possibly proximodistally, in a manner consistent with the patterns of ballistic behavior observed; 3) distribution of sensilla on the original tail will be arranged in a manner consistent with the placement and organization of autotomy planes; and 4) the distribution of the sensilla on the original tail will be denser and more abundant than those on the fully regenerated tail, consistent with the regenerated portion of the tail not being capable of the adaptive responses displayed by the original tail when released (Cooper and Smith, 2009).

To test these predictions, we examined scale size and form, and mapped the density, distribution, and spacing of the cutaneous sensilla of the leopard gecko *E. macularius* (Blyth) 1854 for several regions of the body and tail (Fig. 1), using a similar sampling protocol to that of Matveyeva and Ananjeva (1995), who surveyed the distribution of cutaneous sensilla in 29 species of lizard (18 agamids, eight iguanids, and three gekkotans). Their sampling from the tail was less exhaustive than ours.

MATERIALS AND METHODS

Selection and Processing of Skin Samples

All animal care, handling, and experimentation followed procedures approved by The University of Calgary Animal Care Committee, following Canadian Council on Animal Care guidelines under University of Calgary protocol number BI07R-32. Seven original tails and two fully regenerated (Lynn et al., 2013) tails were removed from specimens (snout-vent length 89–120 mm) of leopard geckos. The original tails were obtained by inducing autotomy, and the regenerated tails were severed from sacrificed individuals. Each tail was divided sagitally into a left and right half, and one half was cut into five segments of equal length, numbered (1–5) from anterior to posterior (Fig. 1a,b). Strips of skin were removed from the central region of each of these segments and cut into five area-equivalent sectors (A–E), from dorsal to ventral (Fig. 1b), transferred to histological tissue baskets (Simport Histosette I, Simport Plastics, Beloeil, Quebec) and stored in 70% ethanol. Surface debris was removed by immersion of the specimen-containing tissue baskets in distilled water in a sonicating bath. Samples were then laid flat, air-dried, and cellophane-stripped (using adhesive tape) to remove remaining surface debris and loose epidermis. Gekkotan sensilla are notoriously difficult to visualize (Matveyeva and Ananjeva, 1995) because the relatively soft nature of the skin often results in the puckering of the outer epidermal generation during preparation for SEM observation. The cleaning of the surface, as described above, enabled us to locate as many sensilla as possible, but resulted in stripping away of most of the filaments carried by bristled sensilla (Fig. 2a). We were able to confirm, through supplemental observations, that the sensilla on the skin surface of the Leopard gecko bear single bristles (as depicted by Hiller, 1971), except for those in the labial region, where nonbristled sensilla are found. The cleaned samples were fully dehydrated by immersion (for 30 min each) in 85% ethanol, 100% ethanol (twice), 25% hexamethyldisalizane (HMDS), 50% HMDS, 75% HMDS, and 100% HMDS (twice), and they were then placed on an absorbent surface (a Kimwipe®) in a fume hood for 10 min, to allow the remaining HMDS to evaporate, and left to air dry overnight. They were then affixed, by double-sided adhesive tape, to 2.54×10.16 cm^2 aluminum plates mounted on aluminum SEM stubs, and sputter coated with gold alloy (2-nm thick gold/palladium film, 82%Au/18%Pd) using a Hummer sputter coater. Skin samples were imaged in an SEI XL 30 ESEM at the Microscopy and Imaging Centre, Faculty of Medicine, University of Calgary.

To compare the density, distribution, and spacing of sensilla on the tail to those on the body, squares or rectangles of skin were excised from various regions of five of the leopard gecko specimens from which the original and regenerated tails were taken. The regions sampled were as follows (Fig. 1a): midline dorsum of the head between the eyes; midline dorsum of the back between the shoulders, and between the hips: midline venter of the head in the gular region; midline venter of the body between the shoulders, and between the hips; dorsum and venter of the thigh, crus and pes; upper labial scales; lower labial scales. These regions were chosen to provide representative coverage of the body surface, and to include areas in which sensilla density may be expected to be particularly high, such as the labial region (Matveyeva and Ananjeva, 1995). All of these samples were processed and imaged identically to the tail samples described above.

Assessing Scale Morphology and Mapping and Counting Sensilla

Matveyeva and Ananjeva (1995) stated that they examined densities of sensilla of different body regions of the iguanid, agamid, and gekkotan taxa that they studied. What was actually done, however, was to record the numbers of sensilla per scale in different body regions. Neither the dimensions of the scales upon which sensilla were located nor the spacing between sensilla within the confines of these scales, were assessed, so calculation and comparison of actual densities of sensilla between body regions was not possible. To overcome this, we recorded the density of sensilla by comparing their number per unit area of skin (sensilla per mm^2), and also recorded scale dimensions and spacing between sensilla, allowing the comparison of distribution and density patterns of sensilla between body regions.

For each area of the body from which samples of skin were harvested, scale form was surveyed. Scale dimensions were recorded by taking two measurements in ImageJ 1.45s (Schneider et al., 2012), representing the longest and shortest dimension at right angles to each other (Fig. 2a). These were used, together with images of the scales, to determine their length to width ratio and general shape. The approximate surface area of each type of scale was calculated from the length and width data, by measuring 10 scales in each focal area and calculating a mean. For each tail segment 50 scales were measured, resulting in 250 scales for each tail as a whole. Using ImageJ 1.45s, the diameters of the sensilla borne on the scales of the skin samples were measured. Fifty sensilla were measured in this way for each sample of skin (tail and body) examined. Thus, for each tail, 250 sensilla were measured in each segment.

For each region of the skin surveyed from the body and tail (Fig. 1), all sensilla were located and counted on SEM images of the samples (6 mm^2 patches for the body) and the density of sensilla per mm^2 calculated. For the original tail, these calculations were made for each segment and its constituent sectors (A–E, Fig. 1b), the scales on the original tail being arranged in whorls, with clear demarcation furrows between them. Several

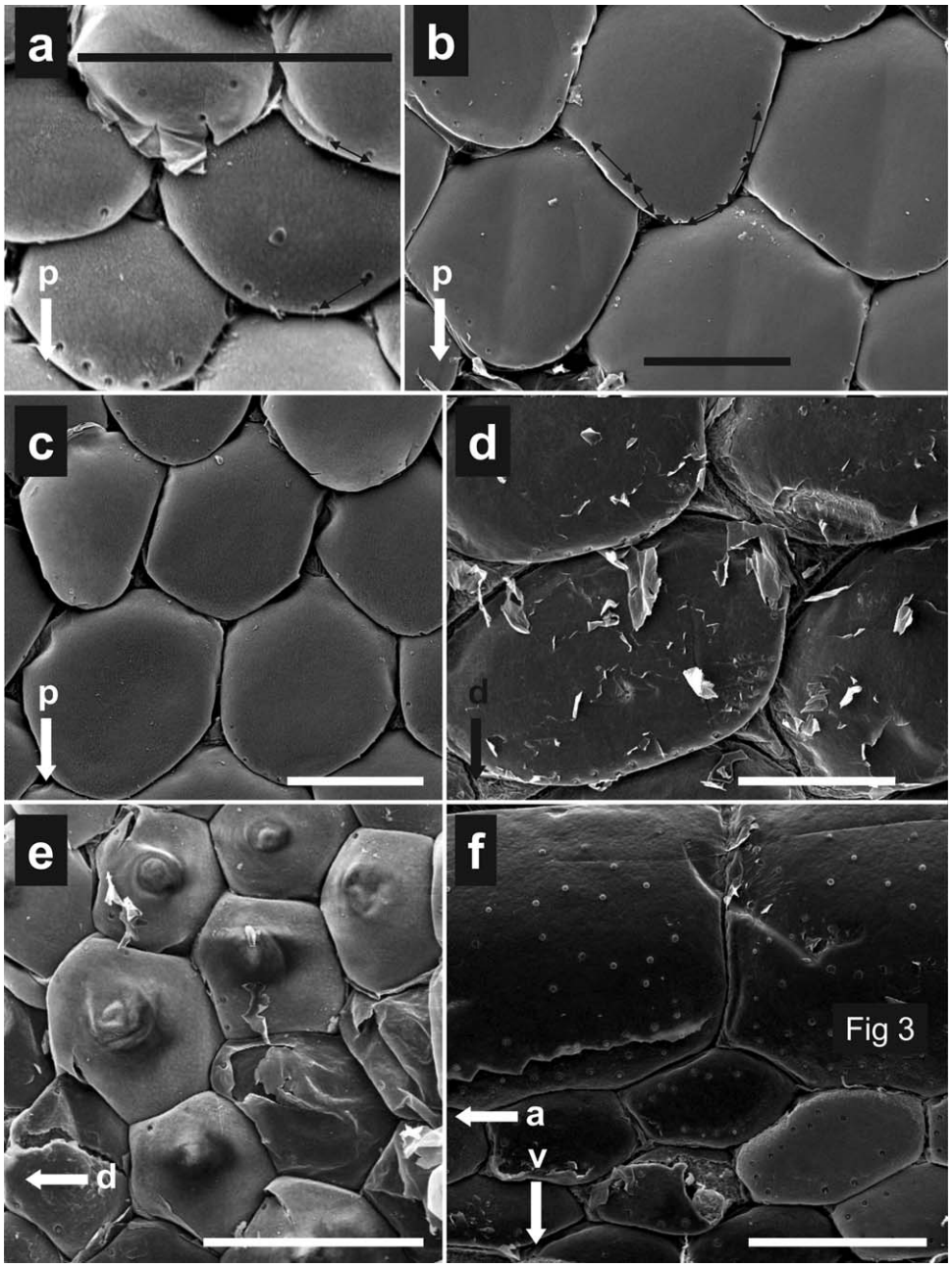

Fig. 3. Scales and their associated sensilla from the ventral regions of the body (see Fig. 1a). (**a**) Gular. The small, black, double-headed arrows indicate how distances between sensilla on scales were measured (from the center of one button to the next). (**b**) Between the shoulders. The small, black, double-headed arrows represent distances as described for panel a. (**c**) Between hips. (**d**) Thigh. (**e**) Pes. (**f**) Lower labial and, to the bottom of the panel, adjoining gular scales. Sensilla are distributed across the surface of the labial scales. Directions are indicated by arrows—a, anterior; d, distal; p, posterior; v, ventral. The scale bar for all panels = 500 μm.

whorls were present in each segment sampled. Similar approaches to the calculation of density and distribution of sensilla were made for equivalently determined segments and sectors of skin of regenerated tails (which show no evidence of whorls of scales).

To determine the relationship between the whorls of the original tail and autotomy planes, preserved leopard gecko specimens were examined. Fine entomological pins were inserted transversely through the mid-point of each whorl, at the dorsal extremity of the tail. These specimens were radiographed using a Kubtec Xpert 80 radiography system, and the location of intervertebral joints and intravertebral autotomy planes mapped in relation to the marker pins.

Distribution of sensilla was also assessed by counting the number of sensilla per scale in each region sampled, and by measuring the distance between adjacent sensilla on individual scales (from the center of the button of one sensillum to that of the next, Fig. 3a,b) to determine, for each region sampled, the average distance between sensilla. Such data were taken from a single individual to avoid variance related to differences in

TABLE 1. Length to width ratios (see Fig. 2) ± sd of each scale type (dimensions in mm) represented in each sampling area (see Fig. 1)

	Scale type	Tubercle	Dorsal	Ventral	Other
Original tail	Segment 1	1.402 ± 0.23	0.819 ± 0.76	1.439 ± 1.06	—
	Segment 2	1.196 ± 0.37	0.616 ± 0.51	1.462 ± 0.90	—
	Segment 3	0.918 ± 0.47	1.361 ± 0.194	1.048 ± 0.48	—
	Segment 4	1.361 ± 0.19	1.266 ± 0.39	1.489 ± 0.29	—
	Segment 5	—	—	—	1.051 ± 0.19
Regenerate tail	Segment 1	—	1.193 ± 0.11	2.353 ± 0.39	—
	Segment 2	—	1.134 ± 0.12	1.934 ± 0.45	—
	Segment 3	—	1.545 ± 0.26	2.289 ± 0.37	—
	Segment 4	—	0.934 ± 0.07	1.288 ± 0.20	—
	Segment 5	—	—	—	0.875 ± 0.15
Dorsal body	Between eyes	1.003 ± 0.02	1.305 ± 0.36	—	—
	Between shoulders	1.013 ± 0.08	1.456 ± 0.29	—	—
	Between hips	1.136 ± 0.03	1.364 ± 0.38	—	—
	Dorsum thigh	1.308 ± 0.19	1.507 ± 0.21	—	—
	Dorsum crus	0.966 ± 0.66	1.231 ± 0.84	—	—
	Dorsum pes	0.999 ± 0.10	0.644 ± 0.18	—	—
	Upper labials	—	—	—	0.941 ± 0.10
Ventral body	Gular	—	—	0.941 ± 0.101.054	—
	Between shoulders	—	—	1.200 ± 0.13	—
	Between hips	—	—	1.262 ± 0.17	—
	Venter thigh	—	—	1.179 ± 0.20	—
	Venter crus	—	—	1.115 ± 0.26	—
	Venter pes	—	—	1.294 ± 0.38	—
	Lower labials	—	—	—	1.744 ± 0.39

Measurements were taken for the longest dimensions of each scale perpendicular to each other. For segment 5 of the tail individual scale types are no longer discernible, although scales here are of variable shapes, so a combined mean value for all scales for this segment is presented.

absolute size between individuals. Distances were examined on other individuals to determine consistency, but are not reported here. In total, 1403 intersensillar distances were measured.

Mapping of Sensilla on the Tail

To obtain an integrated depiction of the distribution of sensilla on the surface of the original tail, SEM photographs of representative sectors from each segment were imported into tpsDig v. 2.16 (Rohlf, 2005), and the bivariate coordinates of each sensillum recorded and plotted.

Determining Patterns of Distribution of Sensilla on the Tail

Sensilla are multiple instantiations of a single developmental feature, and are thus iterative homologs (Ghiselin, 1976; Wagner, 1989, 1994; Roth, 1994). Because sensilla counts were taken for multiple skin samples of each lizard's body and tail (Fig. 1), these data, and the estimates of sensilla density derived from them, are not independent within each lizard. Statistical examination of the distribution patterns of sensilla on the original tails of leopard geckos (the main focus of our study) required accounting for this lack of independence. We subjected the original tail sensilla density data to repeated-measures analysis of variance (Morrison, 1976; Potvin et al., 1990), using proc glm in SAS® 9.3 (SAS Institute, Cary, NC). Each segment was sampled as a block, and each sector's density estimate within the block was treated as a repeated measurement of sensilla density over a particular part of the dorsoventral continuum. The fixed effects were thus segment and sector, and we included an interaction effect between segment and sector. Because we could make no assumptions about the structure of the within-individual variance–covariance matrix of the data (Littell et al., 2000), our initial analysis successively assigned several of the variance–covariance structures most reasonably to be expected for the data (Supporting Information Table S1; Wolfinger, 1996; Littell et al., 2000) to the repeated-measures model. These were evaluated by comparing the sizes of the Akaike information coefficients calculated for each (Wolfinger, 1996), the smallest being selected (Supporting Information Table S1). Differences in density among segments and among sectors within segments were evaluated by means of post hoc Tukey tests carried out within the repeated-measures model using the selected variance–covariance structure.

For other body regions (Fig. 1), sensilla density estimates were averaged for the body of each lizard, because we simply wished to know whether or not sensilla density on the original tail was different from that of the body in general. We did not pose questions about the functional meaning of particular patterns of density and distribution of sensilla of body (as opposed to tail) regions. The pertinent data were pooled, by body and by tail, and compared by means of a Mann-Whitney U-statistic, to explore differences in distribution and central tendency. This method ignores nonindependence of density estimates within the body and within the tail, and takes no account of the variance–covariance structure of the data, but suffices to test for a simple difference between body and tail.

Sensilla density estimates were available for only two regenerated tails, which was insufficient for statistical investigation. These were examined by simple plots and qualitative conclusions drawn.

RESULTS

Scale Descriptions

The dorsal regions of the body (Fig. 1a) are clad in two general types of integumentary derivative, scales (which may be granular, semi-imbricating, or imbricating and which are hereafter referred to simply as scales), and tubercles (Fig. 2a–d). Tubercles vary in size from region to region (Tables 1 and 2). On average, the largest ones are

TABLE 2. Mean areas (mm^2), ±sd of each scale type represented in each sampling area (see Fig. 1)

	Scale type	Tubercle	Dorsal	Ventral	Other
Original tail	Segment 1	0.914 ± 0.08	0.232 ± 0.11	0.575 ± 0.31	—
	Segment 2	0.823 ± 0.07	0.224 ± 0.14	0.545 ± 0.09	—
	Segment 3	0.551 ± 0.12	0.161 ± 0.12	0.575 ±0.61	—
	Segment 4	0.716 ± 0.46	0.127 ± 0.07	0.295 ± 1.49	—
	Segment 5	—	—	—	0.644 ± 0.34
Regenerate tail	Segment 1	—	0.250 ± 0.07	0.892 ± 0.23	—
	Segment 2	—	0.282 ± 0.02	1.031 ± 0.16	—
	Segment 3	—	0.333 ± 0.02	1.292 ± 0.31	—
	Segment 4	—	0.255 ±0.31	1.121 ±0.05	—
	Segment 5	—	—	—	0.761 ± 0.57
Dorsal body	Between eyes	0.644 ± 0.06	0.123 ± 0.06	—	—
	Between shoulders	0.141 ± 0.15	0.142 ± 0.04	—	—
	Between hips	1.434 ± 0.23	0.117 ± 0.05	—	—
	Dorsum thigh	3.092 ± 1.72	0.301 ± −18	—	—
	Dorsum crus	2.473 ± 1.72	0.207 ± 0.07	—	—
	Dorsum pes	1.534 ± 0.36	0.450 ± 0.10	—	—
	Upper labials	—	—	—	2.612 ± 0.16
Ventral body	Gular	—	—	0.246 ± 0.05	—
	Between shoulders	—	—	1.091 ± 0.21	—
	Between hips	—	—	0.948 ± 0.28	—
	Venter thigh	—	—	0.948 ± 0.28	—
	Venter crus	—	—	1.054 ± 0.21	—
	Venter pes	—	—	0.962 ± 1.23	—
	Lower labials	—	—	—	0.369 ± 0.45

For segment 5 of the tail individual scale types are no longer discernible, although scales here are of variable shapes, so a combined mean value for all scales for this segment is presented.

located on the dorsum of the crus and thigh, and the smallest occur on the dorsum of the head, between the eyes (Table 2).

The scales on the dorsal aspect of the body (Fig. 2b,c) are, on average, oblong (Table 1), with their longest dimension oriented transversely, and their shortest dimension orthogonal to this. The long axis/short axis orientation changes with respect to body region, with those on the appendages being oriented with their long axes at right angles to the long axis of the limb (Fig. 2d,e). Like the tubercles, they vary in size from region to region (Table 2), with the smallest located between the hips on the dorsal surface of the body, and the largest located on the dorsum of the pes.

Tubercles generally have, because of their size and shape, a relatively small perimeter in relation to their enclosed area (Fig. 2c), whereas the oblong dorsal scales have a greater length of edge relative to their enclosed area. Tubercles juxtapose neighboring scales and are usually isolated from other tubercles by intervening scales. The dorsal scales have a slightly raised posterior edge (Fig. 2a–c), but essentially juxtapose their neighbors. The scales on the dorsal aspect of the limbs are more imbricating (Fig. 2d,e).

The upper labial scales (Fig. 2f) are the largest of the scales sampled (Table 2), and have an irregularly oblong shape (Table 1, Fig. 2f). They are more nearly square than are the dorsal scales (Table 1). The lower labial scales (Fig. 3f) are similarly shaped to the uppers (Table 1), but have smaller absolute dimensions (Table 2).

Ventral body scales are imbricating (Fig. 3) for all regions sampled (Fig. 1a), although they vary considerably in absolute dimensions (Table 2). They have a rounded to diamond-shaped appearance, and the posterior free edge overlaps neighbors lying laterad and posteriad (Fig. 3a–d). The free trailing edges may be short (Fig. 3a) or moderately long (Fig. 3b,c). As with the dorsal scales, orientation changes with body region, with ventral scales on the appendages (Fig. 3d) being aligned in relation to the long axes of the limb segments. Ventral scales range from being almost "square" (in terms of length to width ratio), as in the gular region (Fig. 3a; Table 1) to distinctly longer than wide, as on the ventral body surface between the hips (Fig. 3c; Table 1). They also vary in size, being smallest in the gular region (Fig. 3a) and largest, on average, on the venter of the crus (Table 2). The ventral regions of the body are devoid of tubercles.

The original tail bears scales arranged in whorls around its circumference (Fig. 4). Radiographic examination reveals that the breadth of each whorl corresponds to the length of an underlying vertebra, indicating a 1:1 correspondence of whorls and autotomy planes. Dorsally each whorl carries relatively small, semi-imbricating scales, the free edges of which are directed posteriorly (Fig. 5a). Interspersed among these are larger tubercles (Fig. 5a), that are spaced dorsoventrally in columns, at relatively regular intervals (Fig. 4). They are located close to the center of each whorl and

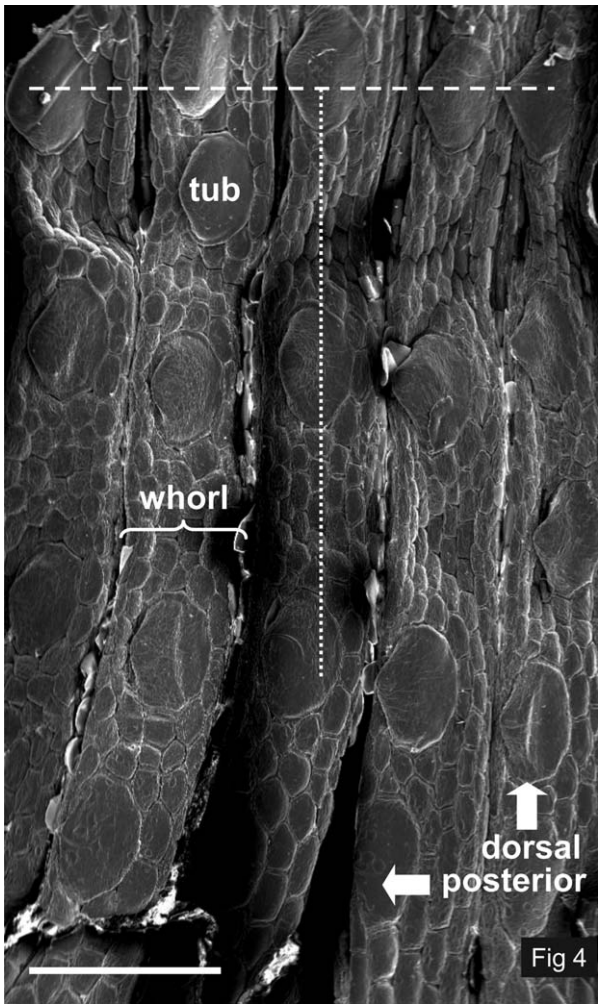

Fig. 4. Skin from one segment of the original tail of the leopard gecko. Whorls of scales, segregated by demarcation lines that are coincident with autotomy planes, are evident. Tubercles (tub) are present on the whorls, and are very prominent dorsally and diminish in prominence ventrally. Tubercles are arranged in columns (vertical dotted line) within whorls, and rows (horizontal dashed line) along the tail. The small, semi-imbricating scales on the dorsal part of the tail merge into broader plates ventrally. Scale bar = 2 mm.

are arranged in longitudinal rows along the length of the tail (Fig. 4).

On the more ventral region of each caudal whorl, the imbricating scales typical of the dorsal region (Fig. 5a,d) give way to polyhedral ventral plates (Figs. 4 and 5c, f) that are markedly broader than long (Table 1). The transition is gradual (Fig. 4), and the tubercles also lose their identity along this transitional gradient.

The sizes of the scales on the tail change along its length, becoming generally smaller more posteriorly (Table 2). The tubercles are generally more oblong (Fig. 4) than they are on the body, as indicated by their length to width ratios (Table 1). Dorsally the semi-imbricating scales of the tail are longer than broad, but they become broader than long more ventrally (Table 1; Fig. 4), as they grade into the ventral plates.

Tubercles on the tail tend to diminish in absolute size from anterior to posterior (Table 2). The ventral plates retain relatively constant average dimensions for the first three segments of the tail (Table 2), and then become markedly smaller.

In the most posterior portion of the tail (segment 5, Fig. 1b), distinction between tubercles, imbricating scales and ventral plates is lost, and scales here are more variable in size but more uniform in shape (Tables 1 and 2).

The regenerated tail lacks tubercles and bears scales that are more homogeneous than those of the original (Fig. 5g). It is clad dorsally and dorsolaterally in rows of semi-imbricating scales of similar size and form to those of the equivalent regions of the original tail (Fig. 5g,h; Tables 1 and 2). In the interstices between these scales, however, reside much smaller scales (Fig. 5g,h), not evident on the original.

Ventrally the regenerated tail bears oblong, juxtaposing, plate-like scales (Fig. 5i) that are moderately to greatly wider than they are long (Table 1), and much larger than the semi-imbricating scales of the dorsal and dorsolateral surfaces (Fig. 5g–i; Table 2).

As for the original tail, the distinction between dorsal and ventral scales becomes much less evident in the region of the tail tip, and that part of the tail carries somewhat squarish (Table 1), juxtaposing scales that are slightly larger than the scales in the equivalent region of the original tail (Table 2).

Distribution and Size of Sensilla

Examination of scales from the regions of the body and tail sampled (Fig. 1) reveals that, in general, cutaneous sensilla are located toward the posterior (distal on the limbs) border of both the scales of the dorsal surface (Figs. 2, 3, and 5), and the plates or imbricating scales of the ventral surface (Figs. 2, 3, and 5). In the case of semi-imbricating and imbricating scales, the sensilla are usually disposed on, or close to, the free distal border (Figs. 2d,e, 3a,b, and 5d,e), often housed in depressions on the trailing edge. Tubercles are either devoid of sensilla or bear relatively few of them (Figs. 5a,b, and 6). On the tail, as tubercles give way to enlarged imbricating scales on the ventrolateral regions, the number of sensilla on such scales increases, and they become more concentrated along the posterior, free edges (Fig. 6).

The pattern outlined above was common across all areas examined except for the labial region and snout. Occasionally scales of the body and tail surface in general have sensilla located on their exposed, broad face (Fig. 5f), but on the labial scales (upper and lower) and on the rostral scales

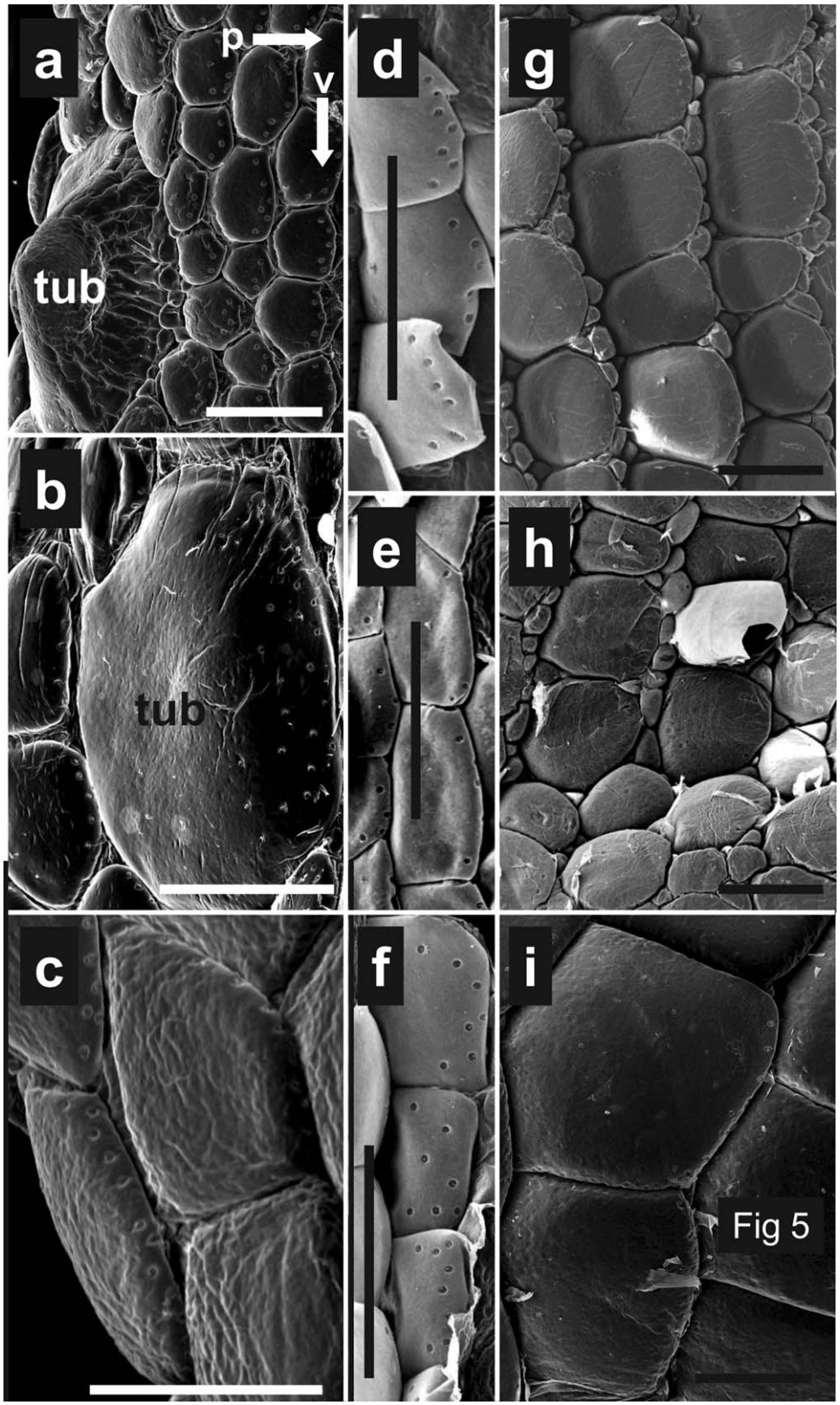

Fig. 5. Scales and their associated sensilla from the original and regenerated tail of the leopard gecko. (**a–c**) Scales from the original tail representing the dorsal (sector A, Fig. 1b), intermediate (sector C, Fig. 1b) and ventral (sector E, Fig. 1b) of a caudal segment, respectively. In (a) and (b) tubercles (tub) are evident, being more prominent and compact in (a). Sensilla are present on the tubercle in the intermediate region (b), but not on the dorsal (a) tubercle. (**d–f**) represent enlarged views of scales represented in panels (a), (b) and (c), respectively. Sensilla are evident on the posterior borders of the scales in (d) and (e), and are present on the broader face of the scales in (f). Panels (**g–i**) show scales from the dorsal (sector A, Fig. 1b), intermediate (sector C, Fig. 1b) and ventral (sector E, Fig. 1b) of a caudal segment, respectively, of a regenerated tail. Small scales are evident intruding between the larger scales in (g) and (h). Directional arrows in panel (a) (p, posterior; v, ventral), apply to all panels. The scale bar for all panels = 500 μm.

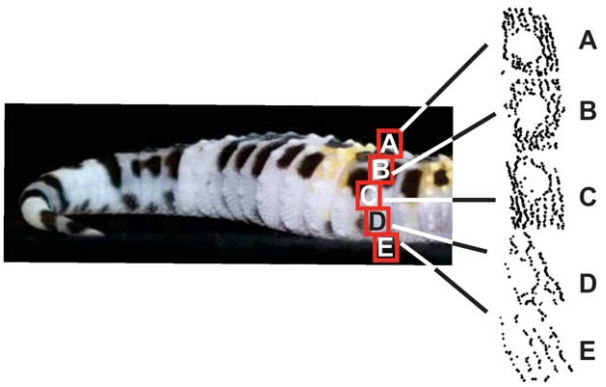

Fig. 6. Composite map (right) of the distribution and placement of sensilla of a single caudal whorl of scales in the anteriormost segment sampled (1—Fig.1b) of the original tail of the leopard gecko. All sensilla in each sector (A–E) were plotted for their bivariate coordinates from SEM images, using tpsDig v.2.16 (see Materials and Methods). The bare gaps in sectors A and B of the coordinate maps represent the location of tubercles, which are devoid of sensilla. In sector C some sensilla are evident on the posterior face of the included tubercle (see Fig. 5b). Sensilla become sparser and more diffuse ventrally, and the tubercles become less evident. The canted alignment of the coordinate maps for sectors D and E results from flattening of the curvature of the tail to produce a planar projection.

lying dorsal to the upper labials, this is much more frequent (Figs. 2f and 3f), and the sensilla are distributed in a somewhat homogeneous pattern, although there is a high concentration of them along the border that impinges upon the rostral (upper labials) and gular (lower labials) scales. The margins of the labial scales that border the mouth are devoid of sensilla. On the body and tail surfaces examined (Fig. 1), the diameter of the cutaneous sensilla is uniform (Supporting Information Table 2).

Density of Sensilla on the Body

On the dorsal body surface, exclusive of the upper labial scales, the highest mean density of sensilla is located on the skin between the hips (Table 3; 33.51/mm^2), and the lowest is encountered on the dorsum of the pes (Table 3; 11.59/mm^2). The upper labial scales exhibit a mean density of sensilla (34.67/mm^2) very similar to that of the dorsal skin between the hips (Table 3), although the sensilla on the dorsal skin are clumped in bands along the posterior edges of the scales (Figs. 2a–c and 3a–d), whereas those of the labial region are arrayed more evenly across the scale surfaces (but do exhibit a greater concentration along their junctions with the rostral and gular scales—Figs. 2f and 3f).

The density of sensilla on the ventral regions of the body is generally noticeably lower than that of the corresponding dorsal areas (Table 3). The lower labial scales are an exception to this (Table 3). The lowest mean density of sensilla on the ventral surface of the body is found on the skin between the hips (mean density 10.41/mm^2), and the highest (apart from the lower labial scales) is located in the gular region (mean density 20.95/mm^2) (Table 3).

Density of Sensilla on the Tail

On the original tail, the density of the sensilla on the dorsal surface (Table 3) is markedly higher than that of any of the sampled region of the dorsal body (Table 4). For sector A, the dorsalmost region of the tail sampled (Fig. 1b), the mean density of sensilla ranges from 59.34 to 76.12/mm^2 (Table 4) for individual segments, compared to mean densities of 34.67 and 33.51/mm^2 for the upper labial scales and the scales between the hips, respectively (Table 3).

For the ventral surface of the tail, sensilla density for sector E (Table 4) ranges from 7.28 to 25.51/mm^2 along the length of the tail, these values being markedly lower than those for the dorsal regions of the same caudal segments. They span a lower range than the densities for the ventral regions of the body (Table 3). In general, sensilla densities for the intervening sectors (B, C, D) of the original tail, along its length, from segment 1 to segment 5 (Table 4), reflect a declining density from dorsal to ventral, although in our sample certain segment/sector combinations exhibit exceptions.

Mean sensilla density on the body is significantly zlower (Mann-Whitney $U < 0.000001$; $P = 0.004483$) and less variable than mean sensilla density on original tails (Fig. 7).

For the regenerated tail (Table 5), the density of sensilla is markedly lower than that for the equivalent regions of the original tail (Table 4). Sector A (segments 1–5) along the length of the regenerated tail exhibits sensilla densities of 4.35–24.65/mm^2, these values falling within, to well below, the sensilla densities exhibited by the dorsal regions of the body and limbs (Table 4). Ventrally the regenerated tail, as represented by sector E (Table 5), registers densities of 2.47–6.34 sensilla/mm^2, well below the lowest densities recorded for the scales on the ventral regions of the body and limbs (Table 3), where the lowest density is 10.41/mm^2, for the ventral scales between the hips.

The repeated-measures model incorporating the antedependence variance–covariance structure displays the lowest Akaike information coefficient (Supporting Information Table S1). This indicates that sensilla densities across the surface of the original tail (as sampled—Fig. 1b) display an autoregressive pattern, and that there is a decline in the strength of this relationship between sampled areas over the surface of the tail with increasing spatial distance (Kenward, 1987;

TABLE 3. Summary statistics for sensilla density (per mm^2) for the dorsal and ventral body surfaces (exclusive of the tail) sampled (see Fig. 1a)

	Between eyes	Between shoulders	Between hips	Dorsum thigh	Dorsum crus	Dorsum pes	Upper labials
N of cases	5	5	5	5	5	5	5
Minimum	17.711	24.948	19.121	16.030	10.639	8.830	31.805
Maximum	29.688	30.650	39.442	23.313	16.206	13.333	37.110
Median	22.503	29.960	35.686	20.268	15.148	11.989	34.858
Mean	24.243	29.057	33.510	20.205	13.737	11.586	34.667
sd.	5.119	2.363	8.212	2.752	2.559	1.686	1.916
	Gular	Between shoulders	Between hips	Ventrum thigh	Ventrum crus	Ventrum pes	Lower labials
N of cases	5	5	5	5	5	5	5
Minimum	17.180	9.081	8.437	10.244	10.414	9.031	31.103
Maximum	28.123	13.134	12.761	17.759	19.455	18.662	34.669
Median	19.191	11.236	10.391	15.603	13.545	17.126	33.124
Mean	20.945	11.287	10.410	14.446	14.667	15.504	32.751
sd.	4.252	1.561	1.735	3.428	3.413	3.834	1.429

Wolfinger, 1996). The existence of a pattern in sensilla densities is thus supported (Fig. 8).

The three fixed effects in the repeated-measures ANOVA are all statistically significant (Supporting Information Table S3). Post hoc Tukey tests indicate no significant differences in least-squares mean sensilla density among segments, with the exception of that between segments two and five (Supporting Information Table S4). The anteroposterior spatial pattern of sensilla density involves a change in the distributions of within-segment dorsoventral densities between segment two and the segments posterior to it; sensilla densities generally decrease dorsally to ventrally in segments three to five, whereas in segment two sensilla densities are similar among sectors, with the exception of the high density of the ventralmost sector (Fig. 8). A simple anteroposterior gradient in sensilla densities over the entire original tail is not confirmed by this analysis; although a subtle

TABLE 4. Summary statistics for sensilla density (per mm^2) for the tail segments sampled (see Fig. 1b) for original tails

	Sector A	Sector B	Sector C	Sector D	Sector E
Segment 1					
Minimum	50.932	48.356	49.399	23.524	5.698
Maximum	78.132	61.393	61.408	49.261	24.448
Median	55.908	50.285	56.277	27.072	20.019
Mean	59.344	51.836	55.039	34.766	17.442
sd.	8.950	4.466	4.340	12.030	6.525
Segment 2					
Minimum	27.673	45.992	44.554	60.292	16.679
Maximum	83.396	85.139	79.909	177.317	25.013
Median	58.916	67.320	68.245	115.857	20.840
Mean	58.827	67.363	63.992	109.871	20.556
sd.	20.348	15.724	12.908	39.352	2.666
Segment 3					
Minimum	35.834	30.553	22.255	10.012	3.671
Maximum	103.487	57.322	51.971	30.811	10.124
Median	73.087	51.971	43.385	23.250	7.750
Mean	66.625	48.094	38.621	21.613	7.284
sd.	24.061	10.338	10.996	6.937	2.226
Segment 4					
Minimum	43.383	84.374	13.749	12.374	8.707
Maximum	98.810	120.580	40.419	35.367	25.262
Median	65.993	117.969	18.273	15.566	11.505
Mean	67.727	108.981	24.487	21.457	15.414
sd.	22.300	15.264	11.121	9.780	6.921
Segment 5					
Minimum	26.208	21.689	17.171	13.104	8.585
Maximum	177.075	148.616	116.996	88.537	60.079
Median	56.549	46.946	37.344	27.741	19.205
Mean	76.123	63.727	48.393	37.806	25.513
sd.	51.999	43.772	34.521	26.093	17.657

For each segment the sensilla densities for sectors A–E (see Fig. 1b) are reported. All data are based upon calculations for seven cases.

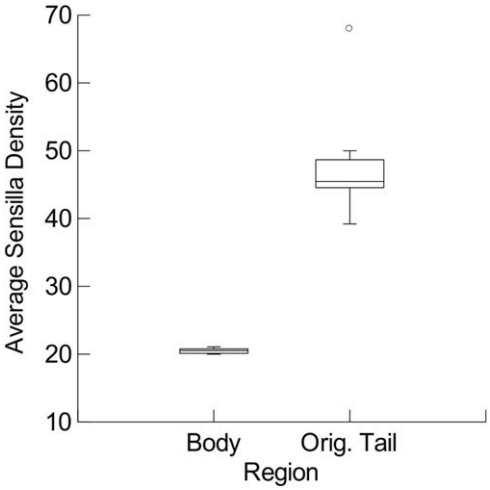

Fig. 7. Box-whisker plots of the pooled mean density (number per mm^2) of sensilla on all regions of the body (left, $n = 5$ animals) and original tail (right, $n = 7$ tails) of the leopard gecko.

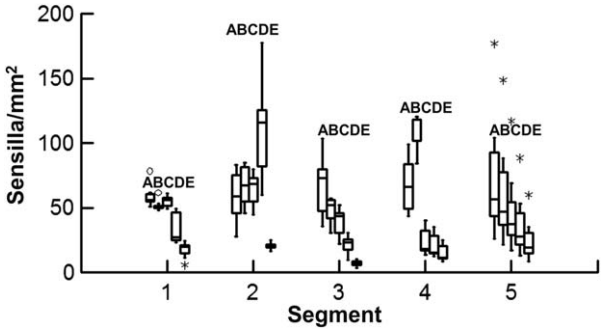

Fig. 8. Box-whisker plots of the density (number per mm^2) of sensilla for all segments (1–5) and sectors (A–E) of the original tail (Fig. 1b) of the leopard gecko ($n = 7$ tails).

sensilla density gradient between segments 2 and 5, sufficient to establish statistically significant differences at these two extremes is evident (Supporting Information Table S3; Fig. 8).

Post hoc Tukey tests for differences among sector sensilla density within segments indicate that virtually all sectors, with the exceptions of adjacent sectors A and B, and C and D, have significantly different least-squares mean sensilla densities around the girth of the entire original tail for all segments. Density rises from the dorsalmost (sector A) to a peak at sector B, then decreases through sectors C and D to a minimum in sector E (Supporting Information Table S5). That intervening adjacent pairs of sectors (B and C and D and E) display significant differences in least-squares mean sensilla density (Supporting Information Table S5) suggests a dorsoventral

TABLE 5. Summary statistics for sensilla density (per mm^2) for the tail segments sampled (see Fig. 1b) for regenerated tails

	Sector A	Sector B	Sector C	Sector D	Sector E
Segment 1					
Minimum	23.717	21.678	11.912	5.151	6.149
Maximum	25.586	22.950	12.189	6.259	6.546
Median	24.651	22.314	12.050	5.705	6.348
Mean	24.651	22.314	12.050	5.705	6.348
sd.	1.322	0.900	0.196	0.784	0.281
Segment 2					
Minimum	3.940	4.409	1.973	0.580	3.597
Maximum	4.757	5.065	6.416	0.726	4.165
Median	4.349	4.737	4.194	0.653	3.881
Mean	4.349	4.737	4.194	0.653	3.881
sd.	0.578	0.464	3.142	0.104	0.402
Segment 3					
Minimum	10.004	8.441	7.177	5.383	4.486
Maximum	10.318	8.523	7.347	7.503	4.533
Median	10.161	8.482	7.262	6.443	4.510
Mean	10.161	8.482	7.262	6.443	4.510
sd.	0.221	0.058	0.120	1.499	0.033
Segment 4					
Minimum	9.487	7.978	5.391	4.959	4.312
Maximum	11.815	9.846	6.892	6.400	5.908
Median	10.651	8.912	6.141	5.680	5.110
Mean	10.651	8.912	6.141	5.680	5.110
sd.	1.646	1.321	1.062	1.019	1.128
Segment 5					
Minimum	12.904	7.997	4.934	2.657	2.277
Maximum	13.328	9.109	6.473	3.427	2.666
Median	13.116	8.553	5.704	3.042	2.471
Mean	13.116	8.553	5.704	3.042	2.471
sd.	0.299	0.786	1.089	0.545	0.275

For each segment the sensilla densities for sectors A–E (see Fig. 1b) are reported. All data are based upon calculations for two cases.

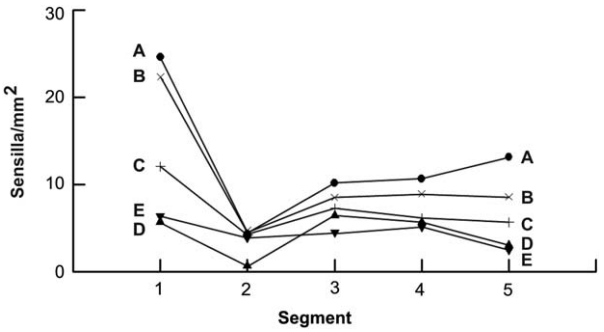

Fig. 9. Representation of the pooled data for the density (number per mm^2) of sensilla for all segments (1–5) and sectors (A–E) of the regenerated tail of the leopard gecko ($n = 2$ tails). Lines trace trends in sensilla density for each sector (A–E) along the length of the tail.

gradient in sensilla density, from higher density dorsally to lower density ventrally, the disposition of the sectors within the segments being slightly incongruent with the slope of the gradient (Fig. 8). The significant interaction effect between segment and sector (Supporting Information Table S5) is produced by the heterogeneity in this dorsal–ventral gradient along the length of the tail (Fig. 8).

In regenerated tails, there is a pattern of relatively high sensilla density in the anteriormost segment, dropping to a low density in the next segment, then rising toward the posterior segment, although not attaining the density of the anteriormost segment (Fig. 9). This pattern is repeated among virtually all of the sectors from segment to segment (Fig. 9). Sectors display a dorsoventral gradient of greater to lesser sensilla density within each segment (Fig. 9). Sensilla densities for regenerated tails (Table 5) are invariably lower than corresponding sensilla densities for original tails (Table 4). For the more distal segments (2–5) of the regenerated tail, density of sensilla is at the level of, or considerably lower than, the densities encountered on the sampled ventral areas of the body (Table 3), and represent the lowest densities of any region of the body surveyed.

Spacing between Sensilla

We here report only spacing between sensilla for scales, because they are generally very sparse, or absent from, tubercles. Measurements of distances between sensilla indicate that, on average, those residing on the dorsal aspects of the original tail are spaced more closely than they are on any other region of the body (Table 6).

Comparison of data for sensilla density (Tables 3–5), average spacing between sensilla (Table 6), and scale size (as represented by scale area—Table 2), indicates that although sensilla may be clustered relatively closely together, as they are on the dorsal scales of the tail (mean distance between the sensilla 64.7 μm), and on the ventral scales between the shoulders (mean distance 65.6 μm), scale size and the number of sensilla per scale ultimately determine sensilla density per unit area. The dorsal scales of the tail carry a modest number of sensilla per scale (Table 6), but the scales themselves are relatively small (Table 2), and the distance between sensilla is also small (Table 6), yielding a high density (Table 4). Conversely, the ventral scales between the shoulders are large (Table 2), and because they carry only a moderate number of sensilla (Table 6), the density in this area is low (Table 3). The dorsal scales between the hips are the smallest of any region sampled (Table 2), and carry more sensilla per scale than do those of the dorsal scales of the original tail (Table 6), although they exhibit a greater average distance between sensilla (Table 6), resulting in a lower density of sensilla per unit area (Table 3).

The ventral region of the original tail (segment 1, sector E—Fig. 1b) bears relatively large scales that, on average, carry about the same number of sensilla as the dorsal scales (Table 6), with an average distance between sensilla (84.1 μm) intermediate between that of the dorsal region of the tail and that of the region carrying the most diffuse sensilla (the dorsal aspect of the crus—Table 6). The overall outcome of this is a relatively low density of sensilla (Table 4).

Our data indicate that counts of sensilla per scale, if considered in isolation from information about scale size, form and intersensillar spacing, are not sufficient to provide a complete picture of their density. The amount of "dead space" in a body region, made up of the broad faces of scales that are devoid of sensilla (Figs. 2–5), together with the shape of the scales (Table 1), determines the edge to surface area ratio, and ultimately the density, of sensilla per unit area. A combination of small, oblong scales carrying closely spaced sensilla provides for high sensilla density, such as is seen on the dorsal surface of the original tail (Table 6).

The regenerated tail exhibits moderate sensilla density on its dorsal aspect (Table 6) at the proximal extremity of the regenerated portion, but this falls quite dramatically further distally (Table 5). Thus, the dorsal aspect of the regenerated tail exhibits mean sensilla densities that, at their highest (Tables 4 and 5), are similar to those on the dorsal region of the head between the eyes (Table 3) and, at their lowest, are similar to, or lower than, the lowest densities encountered on any region of the body sampled (Tables 3 and 4). The ventral aspect of the regenerated tail exhibits by far the lowest density of sensilla/mm^2 of any region surveyed (Tables 3–5), although the average spacing between sensilla, where they occur, is of an intermediate value for all of the areas

TABLE 6. Mean density of sensilla per mm^2 for the areas of skin sampled in this study (non-tuberculate scales), and their relationship to mean distance (in μm) between sensilla, number of sensilla carried per scale, and average scale area for each region

Body region	Sensilla density (mm$^{2)}$	Mean distance between sensilla (μm)	Number of sensilla per scale	Average scale area – rank order from smallest (1) to largest (18) (see Table 2)
Original tail, segment 1, sector A*	59.34	64.7	3–9	5
Upper labials	34.67	92.1	60+	18
Dorsal, between hips	33.51	120.7	10–20	1
Lower labials	32.75	86.2	40+	9
Dorsal, between shoulders	29.06	69.3	2–5†	3
Regenerate tail,segment 1, sector A	24.65‡	90.9	1–8	7
Dorsal, between eyes	24.24	96.8	2–5	2
Gular	20.95	70.4	2–4	6
Dorsal, thigh	20.21	103.4	4–9*	8
Original tail, segment 1, sector E*	17.44	84.1	4–10	11
Ventral, pes	15.50	74.1‡	0–10§	15
Ventral, crus	14.67	71.0	10–14	16
Ventral, thigh	14.47	87.5	4–12	13=
Dorsal, crus	13.74	121.9	1–5	4
Dorsal, pes	11.59	74.6	3–8	10
Ventral, between shoulders	11.29	65.6	4–8	17
Ventral, between hips	10.41	80.9	9–11	13=
Regenerate tail, segment 1, sector E	6.34‡	100.5	3–6	12

Body regions are listed from highest to lowest sensilla density
*Sensilla densities for sectors A and E of the original tail are generally representative of those of other tail segments (see Table 5).
†Some scales in this region may carry a much higher number.
‡The density is highest in Segment A of the regenerated tail. All segments lying posterior to this exhibit much lower densities.
§Many scales in this region are devoid of sensilla, or bear only one sensillum per scale.

surveyed (Table 6), and they are carried on scales of intermediate size (Tables 2, 6).

In some regions spacing between sensilla is relatively small, and yet density is only modest, because sensilla may be absent from many scales, or borne only singly upon scales, thus obviating the possibility of measuring spacing between sensilla within the confines of many of the scales. The ventral aspect of the pes exhibits such a combination (Table 6). Because we restricted ourselves to measuring distances between sensilla on individual scales (Fig. 3b) our statements of distances between sensilla are likely underestimated for areas in which sensilla are sparsely distributed, although our density estimates per unit area, which count all sensilla within a defined patch, are directly comparable for, and representative of, all areas examined. A combination of spacing, sensilla density, and scale size (Table 6) provide the best estimate of the relative mechanoreceptive sensitivity of a particular body region.

DISCUSSION

The complex and varying movements of the detached tail of many geckos (Higham et al., 2013a) have led to the suggestion that perception and integration of external stimuli may be involved (Higham and Russell, 2010, 2012). In squamates, external tactile stimuli are perceived through cutaneous sensilla (Miller and Kasahara, 1967; Hiller, 1978), and the distribution and placement of these structures has been associated with the registering of mechanical contact, and with response to this (Bauer and Russell, 1988; Lauff et al., 1993). It is, therefore, reasonable to infer that variation in density and arrangement of such sensilla across the body surface (Bauer and Russell, 1988) is associated with regional sensitivity.

Our interpretation of the bristle-bearing sensilla, distributed widely across the body and tail of the leopard gecko, as mechanoreceptive structures is predicated upon several lines of evidence. Hiller (1978) demonstated such structures to be mechanoreceptive in agamid lizards. Povel and Van Der Kooij (1996) showed that similarly structured sensilla of the file snake exhibit deposits of glycogen in their discoidal nerve endings, a feature typical of tactile sense organs. Röll (1995) associated the high degree of sensitivity to touch displayed by the gekkotan lizard *Sphaerodactylus cinereus* with a high density of bristled sensilla on the tail and feet. Furthermore, long-established mechanosensory function (Barnes, 1931; Pflüger, 1980; Solon and Kass-Simon, 1981) is evident for analogous and very similarly structured (Darby, 1982; Figs. 5E and 6D) cutaneous receptors of arthropods, provides supporting evidence that the form of squamate bristled sensilla is wholly consistent with mechanoreceptive function. Such Type I receptors of arthropods may, on occasion, have additional sensory modalities, but are always mechanoreceptive (McIver, 1975). Indeed, in thysanuran insects mechanoreceptive bristled sensilla along the caudal filament have been associated with predator avoidance, and the autotomizable

caudal filament has been likened to the breakable tails of lizards (Sharov, 1966; Edwards and Reddy, 1986).

Differential patterns of the distribution of sensilla have long been noted (Leydig, 1868; Cartier, 1872; Schmidt, 1912, 1913; Priess, 1922), and functional correlates of this have been suggested (Jackson, 1977; Oreyas-Miranda et al., 1977; Jackson and Sharawy, 1980; Maclean, 1980; Stovall, 1985; Lauff et al., 1993: Matveyeva and Ananjeva, 1995; Nikitina and Ananjeva, 2005). However, little more than general inferences about enhanced tactile sensitivity have been advanced.

For *E. macularius*, we found that the highest density of sensilla is located on the dorsal and lateral aspects of the original tail, and that a gradient to relatively low densities on the underside of the tail is evident. We thus suggest that the pattern of density of sensilla on the tail is consistent with the means of mediation of the complex behaviors of the autotomized tails of geckos, and also with how the precise location at which caudal autotomy takes place may be determined in instances in which a predator makes contact with the tail. Such findings open the door for future comparative studies that explore the link between scale and sensillar morphology on the one hand and tail function on the other.

With regard to our predictions, we found that 1) the density patterns and distribution of sensilla on the original tail, relative to those on the body, are consistent with the tail being a structure with enhanced sensitivity, and that this, in turn, is consistent with the detached tail being able to undergo highly variable activity patterns following release (Higham and Russell 2010, 2012); 2) sensilla distribution on the original tail exhibits a dorsoventral gradient in density that is consistent with ballistic behavior of the detached tail; 3) the distribution of sensilla on the original tail is apportioned into whorls of scales which are aligned with autotomy planes; and 4) the regenerated tail exhibits a very different pattern of distribution and density of cutaneous sensilla compared to the original, consistent with its reduced ability to be autotomized and to engage in the complex behaviors typical of the original (Cooper and Smith, 2009). We consider the implications of these findings in more depth below.

The density of sensilla per unit area of the skin, and the size and form of the scales that carry them, should inform us about the relative sensitivity of particular areas of the body, and the ways in which that sensitivity can be recruited and permutated. Sherbrooke and Nagle (1996) identified multiscale complexes of receptor-bearing scales in *Phrynosoma*, segregated by zones that lack sensilla, and inferred that groups of scales may act together to receive, register, and transmit stimuli.

As is the case for other regions of the body, there is a higher density of sensilla on the dorsal regions of the tail than on the ventral ones (Tables 3, 4, and 6; Fig. 6). On the tail (Figs. 6 and 8), the dorsoventral differential in the density of sensilla is very marked, and is consistent with input signals emanating from the sensilla being able to provide regionally differentiated proprioceptive input.

Scale form varies across the tail (Hiller, 1971), and the placement of sensilla is largely confined to scale edges (Miller and Kasahara, 1967; Hiller, 1971; Sherbrooke and Nagle, 1996; Nikitina and Ananjeva, 2005). Scale margins are likely to impinge upon adjacent areas of the tail, and upon features of the physical environment. Such contact results in discharge of the nerves associated with the sensilla (Russell and Bauer, 1987; Lauff et al., 1993). The dorsal and lateral regions of the original tail bear small, imbricating scales with a high density of sensilla on their free, trailing edges. This combination of features provides for increased local sensitivity.

Observations of the postautotomic movements of the leopard gecko tail reveal that rapid rhythmic swings are initiated immediately, and that these induce the tail to travel extensively within its own local environment (Higham and Russell, 2012). As it does so, it generally remains dorsal side uppermost, with its ventral surface, bearing less densely packed sensilla (Table 4), contacting the substratum. Occasionally, the tail may roll or invert. If it does so, the densely packed sensilla on the dorsal and lateral surfaces will become simultaneously, rather than unilaterally, compressed, as is the case in rhythmic swings. Such a shift in mechanoreceptive input could trigger a righting response, brought about by alterations in the contraction patterns of the tail muscles. The mechanisms underlying the righting response require further investigation, which could be undertaken by simultaneously recording the activity patterns of sensory neurons associated with the dorsal sensilla and the activity patterns of the muscles associated with them. Upon righting, the left–right rhythmic swings resume, indicative that the pattern of sensory input reverts back to its initial condition.

The distribution pattern of the sensilla on the original tail is also consistent with the thrusting responses that occur when the detached tail makes contact with objects encountered with its lateral surface, as was the case with contact with the walls of the experimental arena used by Higham and Russell (2010, 2012). Contact unilaterally with the arena wall would result in increased levels of deformation of the more densely aggregated sensilla on one side of the dorsolateral region of the tail, likely invoking a higher intensity of muscle contraction on that side, resulting in a thrusting of the tail away from contact. Once free of

such contact, the tail resumes its rhythmic swinging (Higham and Russell, 2010, 2012).

Ballistic jumps and flips of the detached original tail are brought about by simultaneous contraction of muscles on the left and right sides of the tail (Higham and Russell, 2012, resulting in its dorsoventral, rather than left–right, bending and the launching of the tail away from the surface (Higham and Russell, 2012). These bilateral muscle contractions are more intense than those responsible for rhythmic swinging (Higham and Russell, 2012). No consistent association has yet been made between changed patterns of contact with the external environment and the periodicity of these ballistic movements, so the trigger for them remains elusive (Higham and Russell, 2012).

The density and distribution of sensilla on the original tail may also be associated with determining where along the length of the tail autotomy will take place, and thus which autotomy plane is called into action. The scales of the original tail, and thus the sensilla that they carry, are arranged in whorls (Fig. 4), and these bear a one-to-one relationship with autotomy planes. The boundaries between whorls provide for weakened areas at which skin breakage occurs during autotomy (Gilbert et al., 2013).

Although previous experimental work (Higham and Russell, 2010, 2012; Higham et al., 2013a) has focused upon maximal autotomy of the tail, it is well established that the tail is capable of breaking at any point along its length where autotomy planes are situated (Fleming et al., 2013), and that economy of autotomy (shedding the smallest amount of tail possible) might be practiced. The regulation of how and where the break takes place is not understood, but physical contact of the tail by a predator may determine the site of breakage (Woodland, 1920; Higham et al., 2013b). Fracture at a particular autotomy plane could be mediated through the sensilla on the tail. Squamate mechanoreceptors are phasic-tonic (Hiller, 1978) and fire quickly in response to a stimulus. The high density of sensilla on the dorsal and lateral regions of the original tail, and their segregation into zones represented by whorls, is consistent with the provision of rapid and local conduct of messages to the spinal cord. Local and focused neural input, as a result of predator contact, could reflexively induce the instantaneous spasmodic contraction of caudal muscles (Werner, 2008) in the immediate vicinity of a particular whorl, thereby promoting breakage at a specific and appropriate point.

Response is graded according to stimulus intensity (Lauff et al., 1993), and the number of sensilla stimulated would be important in determining the level of response. In accordance with this, stimuli of lesser intensity could be responsible for the occurrence of partial tail breakages that lead to incomplete autotomy and the formation of bifid or trifid tails (Sood, 1939; Evans and Bellairs, 1983) that consist of a retained original tail and one or more regenerates growing from the location of the incomplete break.

Investigation of neural circuitry in relation to integumentary whorls and autotomy planes will likely be instructive in understanding how economy of autotomy is affected. One way to approach this is through sensory ablation. If the ability of sensory receptors to convey information from the environment (e.g., predator's jaws) was eliminated, then the lizard may not drop the appropriate length of tail. Ablating sensory feedback would also provide a means of determining the functional role of the sensory receptors during dynamic postautotomic behaviors. Overall, investigation of the neural circuitry of the original tail will be instructive in determining the relationship between our morphological findings and the means by which both the site of autotomy and the behavior patterns of the released tail are regulated.

In contrast to the original tail, the regenerated tail is much less well endowed with sensilla (Tables 4 and 5), is not segmentally arranged (Gilbert et al., 2013), and lacks autotomy planes. Thus, it cannot be broken within its own length. The scale and sensilla patterns that characterize the original tail (Tables 1, 2, and 4) differ considerably from those of the regenerated structure (Tables 1, 2, and 5). This suggests that the integumentary features of the original tail are adaptively associated with the localization of sensory perception in relation to the site of autotomy, and activities and responses of the tail immediately following its detachment. None of these roles are attributable to the regenerated components of the tail.

Our findings concerning distribution and density patterns of sensilla on the tail of the leopard gecko corroborate the observations of Matveyeva and Ananjeva (1995) that the tail has the highest density of any region of the body. We relate these findings to the regional differentiation of scale form, spacing between sensilla and density of sensilla per unit area. Furthermore, we demonstrate that the distribution of caudal sensilla exhibits a dorsoventral gradational pattern, and that they are present as fields carried upon the whorls of scales that characterize the original tail. As such, the arrangement of caudal sensilla is topographically related to the arrangement of caudal autotomy planes. We provide functional interpretations for the arrangement of sensilla on the tail, and suggest experimental ways of testing them.

Caudal autotomy is widespread among lizards (Higham et al., 2013b), and tail form and function are very variable. Approaches to mapping the distribution of sensilla on tails of differing form, relating these patterns to scale form, and the documentation of both the stimuli that lead to autotomy (Fox et al., 1998) and the postautotomic

behavior of such tails will help to elucidate the relationship between cutaneous sensitivity and patterns of autotomy. Exploration of the neural circuitry and neural functioning of such tails will further contribute to our understanding of the process of autotomy and the way the tail acts after being released.

Our focus herein has been on caudal autotomy, but it is important to recognize that the tail plays roles in locomotion while still attached to the body. We know nothing about sensory feedback from the tail during various locomotor actions and responses, and future investigation should therefore bear such factors in mind as well. Additionally, it is evident that lineage-based differences may be present in the prevalence of cutaneous mechanoreceptors, so comparisons should also consider phylogenetic relationships. For example, Matveyeva and Ananjeva (1995) noted that the density of sensilla, for comparable body regions, is generally much higher in iguanids and gekkotans than it is in agamids.

ACKNOWLEDGMENTS

The Microscopy and Imaging Facility, Faculty of Medicine, University of Calgary facilitated the SEM work. The authors thank two anonymous reviewers whose comments allowed us to improve this contribution.

LITERATURE CITED

Ananjeva NB, Dilmuchamedov ME, Matveyeva TN. 1991. The skin sense organs of some iguanian lizards. J Herpetol 25: 186–199.

Arnold EN. 1984. Evolutionary aspects of tail shedding in lizards and their relatives. J Nat Hist 18:127–169.

Audy JR. 1953. Strolling on the ceiling. Malayan Nat J 7:182–190.

Bailey SER. 1969. The responses of sensory receptors in the skin of the green lizard *Lacerta viridis* to mechanical and thermal stimulation. Comp Biochem Physiol 29:161–172.

Barnes TC. 1931. Kinesthetic sense of insects. Ann Entomol Soc Am 24:824–826.

Bauer AM, Russell AP. 1988. Morphology of gekkonid cutaneous sensilla, with comments on function and phylogeny in the Carphodactylini (Reptilia: Gekkonidae). Can J Zool 66:1583–1588.

Bellairs Ad'A, Bryant SV. 1985. Autotomy and regeneration in reptiles. In: Gans C, Billet F, editors. Biology of the Reptilia, Vol. 15. New York: Wiley. pp 301–410.

Brown TG. 1911. The intrinsic factors in the act of progression in the mammal. Proc R Soc London B 84:308–319.

Bustard HR. 1968. Temperature dependent tail autotomy mechanisms in gekkonid lizards. Herpetologica 24:127–136.

Cartier O. 1872. Studien über den feineren Bau der Epidermis bei den Geckotiden. Verhandl Physik-med GesellWürzburg 3: 281–301.

Chevalier S, Ijspeert AJ, Ryczko D, Nagy F, Cabelguen JM. 2008. Organisation of the spinal central pattern generators for locomotion in the salamander: Biology and modeling. Brain Res Rev 57:147–161.

Clark DR Jr. 1971. The strategy of tail autotomy in the ground skink *Lygosoma laterale*. J Exp Zool 176:295–302.

Cooper WE Jr, Smith CS. 2009. Costs and economy of autotomy for tail movement and running speed in te skink *Trachylepis maculilabris*. Can J Zool 87:400–406.

Daniels CB. 1985. Economy of autotomy as a lipid conserving mechanism: An hypothesis rejected for the gecko *Phyllodactylus marmoratus*. Copeia 1985:468–472.

Darby CD. 1982. Structure and function of cuticular sensilla of the lobster *Homarus americanus*. J Crustacean Biol 2:1–21.

Eckert R, Randall D, Augustine G. 1988. Animal Physiology—Mechanisms and Adaptations, 3rd ed. New York: W.H. Freeman. xxi + 683p.

Edwards JS, Reddy GR. 1986. Mechanosensory appendages and giant interneurons in the Firebrat (*Thermobia domestica*, Thysanura): A prototype system for terrestrial predator evasion. J Comp Neurol 243:535–546.

Eisthen HL, Braun CB. 2001. Sensors of external conditions in vertebrates. Encyclopedia Life Sci 17:93–101.

Evans SE, Bellairs A d'A. 1983. Histology of a triple tail regenerate in a gecko, *Hemidactylus persicus*. Br J Herpetol 6:319–322.

Fleming PA, Valentine LE, Bateman PW. 2013. Telling tails: Selective pressures acting on investment in lizard tails. Physiol Biochem Zool 86:645–658.

Fox SF, Conder JM, Smith AE. 1998. Sexual dimorphism in the ease of tail autotomy: *Uta stansburiana* with and without previous tail loss. Copeia 1998:376–382.

Ghiselin MT. 1976. The nomenclature of correspondence: A new look at "homology" and "analogy." In: Masterton RB, Hodos W, Jerison H, editors. Evolution, Brain and Behavior: Persistent Problems. Toronto, ON, Canada: Lawrence Erlbaum Associates Publishers. pp 129–142.

Gilbert EAB, Payne SL,Vickaryous MK. 2013. The anatomy and histology of caudal autotomy and regeneration in lizards. Physiol Biochem Zool 86:631–644.

Gottschall JS, Nicholls TR. 2007. Head pitch affects muscle activity in the decerebrate cat hindlimb during walking. Exp Brain Res 182:131–135.

Harris-Warrick RM, Johnson BR. 1989. Motor pattern networks: flexible foundations for rhythmic pattern production. In: Carew TJ, Kelley DB, editors. Perspectives in Neural Systems and Behavior. New York: Liss. pp 51–71.

Harris-Warrick RM, Marder E. 1991. Modulation of neural networks for behavior. Ann Rev Neurosci 14:39–57.

Haupt J, Coineau Y. 1978. Moulting and morphogenesis of sensilla in a prostigmate mite (Acari, Actinotrichida, Actinedida, Caeculidae). I. Mechanoreceptive bristles. Cell Tissue Res 186:63–79.

Higham TE, Russell AP. 2010. Flip, flop and fly: Modulated motor control and highly variable movement patterns of autotomized gecko tails. Biol Lett 6:70–73.

Higham TE, Russell AP. 2012. Time-varying motor control of autotomized leopard gecko tails: Multiple inputs and behavioral modulation. J Exp Biol 215:435–441.

Higham TE, Lipsett KR, Syme DA, Russell AP. 2013a. Controlled chaos: Three-dimensional kinematics, fiber histochemistry, and muscle contractile dynamics of autotomized lizard tails. Physiol Biochem Zool 86:611–630.

Higham TE, Russell AP, Zani PA. 2013b. Integrative biology of tail autotomy in lizards. Physiol Biochem Zool 86:603–610.

Hiller U. 1968. Untersuchungen zum Feinbau und zur Funktion der Haftborsten von Reptilien. Zeitschrift Morphol Tiere 62:307–362.

Hiller U. 1971. Form und Funktion der Hautsinnesorgane bei Gekkoniden. 1. Licht- und rasterelektronmikroskopische Untersuhungen. Forma Functio 4:240–253.

Hiller U. 1976. Ultrastructure and regeneration of cutaneous sensilla in gekkonid lizards. In: Ben Shaul Y, editor. Proceedings of Sixth European Congress on Electron Microscoscopy. Jerusalem: Tal International Publishers, Vol. 1: pp 77–78.

Hiller U. 1978. Morphology and electrophysiological properties of cutaneous sensilla in agamid lizards. Pflügers archiv 377:189–191.

Iggo A. 1982. Cutaneous sensory mechanisms. In: Barlow HB, Mollen JD, editors. The Senses. Cambridge: Cambridge University Press. pp 369–408.

Jackson MK. 1977. Histology and distribution of cutaneous ttouch corpuscles in some leptotyphlopid and colubrid snakes (Reptilia, Serpentes). J Herpetol 11:7–15.

Jackson MK, Sharawy M. 1980. Scanning electron microscopy and distribution of specialized mechanoreceptors in the Texas rat snake, *Elaphe obsoleta lindheimeri*. J Morphol 163:59–67.
Kenward MG. 1987. A method for comparing profiles of repeated measurements. J R Stat Soc C (Appl Stat) 36:296–308.
Landmann L., 1975. The sense organs in the skin of the head of Squamata (Reptilia). Israel J. Zool. 24:99–135.
Lauff RF, Russell AP, Bauer AM. 1993. Topography of the digital cutaneous sensilla of the Tokay gecko, *Gekko gecko* (Reptilia, Gekkonidae) and their potential role in locomotion. Can J Zool 71:2462–2472.
Leydig F. 1868. Über Organe eines sechsten Sinnes. Dresden: E. Blochmann and Sohn.
Littell RC, Pendergast J, Natarajan R. 2000. Modelling covariance structure in the analysis of repeated measures data. Stat Med 19:1793–1819.
Lynn SE, Borkovic BP, Russell AP. 2013. Relative apportioning of resources to the body and regenerating tail in juvenile Leopard geckos (*Eublepharis macularius*) maintained on different dietary rations. Physiol Biochem Zool 86:659–668.
Maclean S. 1980. Ultrastructure of epidermal sensory receptors in *Amphibolurus barbatus* (Lacertilia : Agamidae). Cell Tissue Res 210:435–445.
Maderson PFA. 1965. The structure and development of the squamate epidermis. In: Lyne AG, Short BF, editors. Biology of the Skin and Hair Growth. New York: American Elsevier Publishing Company. pp 129–153.
Mahendra BC. 1936. Contributions to the bionomics, anatomy, reproduction and development of the Indian house-gecko, Hemidactylus flaviviridis Ruppel. Part I. Proc Indian Acad Sci B 4:250–281.
Matveyeva TN, Ananjeva NB. 1995. The distribution and number of the skin sense organs of agamid, iguanid and gekkonid lizards. J Zool (London) 235:253–268.
McIver SB. 1975. Structure of cuticular mechanoreceptors of arthropods. Ann Rev Entomol 20:381–397.
Medel RG. 1992. Cost and benefits of tail loss: Assessing economy of autotomy in two lizard species of central Chile. Revista Chilena Historia Nat 65:357–361.
Miller MR, Kasahara M. 1967. Studies on the cutaneous innervation of lizards. Proc Calif Acad Sci 54:549–568.
Morrison DF. 1976. Multivariate Statistical Methods, 2nd ed. Toronto, ON, Canada: McGraw-Hill Book Co. xv + 415p.
Nikitina NG, Ananjeva NB. 2005. The skin sense organs of lizards of *Teratoscincus g*enus (Squamata: Sauria: Gekkonidae). In: Ananjeva N, Tsinenko O, editors. Herpetologia Petropolitana. Proceedings of the 12th Ordinary General Meeting of the Societas Europaea Hepetologica, Vol. 12. St. Petersburg: Russian Journal of Herpetology. August 12–16, 2003. pp 291–295.
Oreyas-Miranda B, Zug GR, Garcia DY, Achaval F. 1977. Scale organs on the head of Leptotyphlops (Reptilia, Serpentes): A variational study. Proc Biol Soc Washington 90:209–213.
Pflüger H-J. 1980. The function of hair sensilla on the locust's leg: The role of tibial hairs. J Exp Biol 87:163–175.
Potvin C, Lechowicz MJ, Tardif S. 1990. The statistical analysis of ecophysiological response curves obtained from experiments involving repeated measures. Ecology 71:1389–1400.
Povel D, Van Der Kooij J. 1996. Scale sensillae of the file snake (Serpentes: Acrochordidae) and some other aquatic and burrowing snakes. Neth J Zool.47:443–456.
Priess F. 1922. Uber Sinnesorgane in der Haut einiger Agamiden Zugleich ein Beitrag zur Phylogenie der Saugtierhaare. Jena Zeitschrift Naturwiss 58:25–76.
Rohlf FJ. 2005. tpsDig, Digitize Landmarks and Outlines, Version 2.05. Stony Brook: Department of Ecology and Evolution, State University of New York at Stony Brook.
Röll B 1995. Epidermal fine structure of the toe tips of *Sphaerodactylus cinereus* (Reptilia, Gekkonidae). J Zool London 235:289–300.
Roth VL. 1994. Within and between organisms: replicators, lineages and homologues. In: Hall BK, editor. Homology. The Hierarchical Basis of Comparative Biology. New York: Academic Press. pp 301–337.
Rumping JM, Jayne BC. 1996. Muscle activity in autotomized tails of a lizard (*Gekko gecko*): A naturally occurring spinal preparation. J Comp Physiol A 17:525–538.
Russell AP, Bauer AM. 1987. Caudal morphology of the knob-tailed geckos, genus *Nephrurus* (Reptilia: Gekkonidae), with special reference to the tail tip. Aust J Zool 35:541–551.
Sane SP, McHenry MJ. 2009. The biomechanics of sensory organs. Integr Comp Biol 49:i8–i23.
Schleich H-H, Kästle W. 1986. Ultrastrukturen an Gecko-Zehen (Reptilia: Sauria: Gekkonidae). Amphibia-Reptilia 7:141–166.
Schmidt WJ. 1912. Studien am Integument der Reptilien. I. Die Haut der Geckoniden. Zeitschrift wissenschaft Zool 101:139–248.
Schmidt WJ. 1913. Studien am Integument der Reptilien. IV. Uroplatus fimbriatus (chneid.) und die Geckoniden. Zool Jahrbuch 36:377–464.
Schneider CA, Rasband WS, Eliceiri KW. 2012. NIH Image to ImageJ: 25 years of image analysis. Nat Methods 9:671–675.
Sharov AG. 1966. Basic Arthropodan Stock with Special Reference to Insects. Oxford: Pergamon Press. xii + 271p.
Sherbrooke WC, Nagle RB. 1996. *Phyrnosoma* intraepidermal receptor: A dorsal intraepidermal mechanoreceptor in horned lizards (*Phrynosoma*, Phrynosomatidae, Reptilia). J Morphol 228:145–154.
Solon MH, Kass-Simon G. 1981. Mechanosensory activity of hair organs on the chelae of *Homarus americanus*. Comp Biochem Physiol 68A:217–223.
Sood MS. 1939. A peculiar case of caudal abnormality in Hemidactylus flaviviridis Rüppel. Proc Indian Acad Sci 9:316–322 + 1 plate.
Stewart GR, Daniel RS. 1975. Microornamentation of lizard scales: Some variations and taxonomic correlations. Herpetologica 31:117–130.
Stewart WJ, Cardenas GS, McHenry MJ. 2013. Zebrafish larvae evade predators by sensing water flow. J Exp Biol 216:388–398.
Stovall RH. 1985. Cephalic scale pits observed on the lizard, *Uta stansburiana*: Light and scanning electron microscopy. J Herpetol 19:425–428.
Todaro F. 1878. Sulla struttura intima della pille de rettili. Atti della Accademia Lincei, Memoire. No. 2.
Wagner GP. 1989. The biological homology concept. Ann Rev Ecol Syst 20:51–69.
Wagner GP. 1994. Homology and the mechanisms of development. In: Hall BK, editor. Homology: The Hierarchical Basis of Comparative Biology. New York: Academic Press. pp 273–299.
Walters BD, Albert PJ, Zacharuk RY. 1998. Morphology and untrastructure of sensilla on the proboscis of the spruce budworm, *Choristoneura fumiferana* (Clem.) (Lepidoptera : Tortricidae). Can J Zool 76:466–479.
Werner YL. 1964. Frequencies of regenerated tails and structure of caudal vertebrae in Israeli desert geckos (Reptilia: Gekkonidae). Isr J Zool 13:134–136.
Werner YL. 1968. Regeneration frequencies in geckos of two ecological types (Reptilia; Gekkonidae). Vie et Milieu Serie c Biol Terrestre 19:199–222.
Werner YL. 2008. Tales of tails. Gekko 5:6–18.
Whelan PJ. 2010. Shining light into the black box of spinal locomotor networks. Philos Trans R Soc London B 365:2383–2395.
Whimster IW. 1980. Neural induction of epidermal sensory organs in gecko skin. In: Spearman RI, Riley PA, editors. The Skin of Vertebrates. Linnean Society Symposium Series No. 9. London: Academic Press. pp 161–167 + 12 plates.
Wolfinger RD. 1996. Heterogeneous variance: covariance structures for repeated measures. J Agric Biol Environ Stat 1:205–230.
Woodland WNF. 1920. Some observations on caudal autotomy and regeneration in the gecko (*Hemidactylus flaviviridis*, Rüppel), with notes on the tails of *Sphenodon* and Pygopus. Q J Microsc Sci 2:63–100.
Yakovenko S, McCrea DA, Stecina K, Prochazka A. 2005. Control of locomotor cycle duration. J Neurophysiol 94:1057–1065.
Zacharuk RY, Shields VD. 1991. Sensilla of immature insects. Ann Rev Entomol 36:331–354.
Zimmermann M. 1986. Neurophysiology of sensory systems. In: Schmidt RF, editor. Fundamentals of Sensory Physiology, 3rd ed. Berlin: Springer Verlag. pp 68–116.